

FMM accelerated BEM for 3D Laplace & Helmholtz Equations

Nail A. Gumerov and Ramani Duraiswami

Institute for Advanced Computer Studies, University of Maryland, College Park, MD 20742

Abstract

We describe development of a fast multipole method accelerated iterative solution of boundary element equations for large problems involving hundreds of thousands elements for the Laplace and Helmholtz equations in 3D. The BEM requires several approximate computations (numerical quadrature, approximations of the boundary shapes using elements) and the convergence criterion for iterative computation. When accelerated using the FMM, these different errors must all be chosen in a way that on the one hand excess work is not done and on the other that the error achieved by the overall computation is acceptable. We show results of developed and tested solvers for the boundary value problems for the Laplace and Helmholtz equations using the BEM/GMRES/FMM. The performance tests for both were conducted in the range $N \lesssim 10^6$ and $kD \lesssim 150$ (in the Helmholtz case) and showed good performance close to theoretical expectations.

1 Introduction

For many problems boundary integral (or element) methods have long been considered as very promising. They can handle complex shapes, lead to problems in boundary variables alone, and lead to simpler meshes as the boundary alone must be discretized rather than the entire domain. Despite these advantages, one issue that has impeded their widespread adoption of these methods is that the integral equation techniques lead to linear systems with dense and possibly non-symmetric matrices, for which efficient iterative solvers may not be available. For problems with N unknowns this requires storage of $O(N^2)$ elements of these matrices. The computation of the individual matrix elements is expensive requiring quadrature of singular or hypersingular functions. To reduce the singularity order and achieve symmetric matrices, many investigators employ Galerkin techniques, which lead to further $O(N^2)$ integral computations. Direct solution of the linear systems has an $O(N^3)$ cost. Use of iterative methods can reduce the cost to $O(N_{iter}N^2)$ operations, where N_{iter} is the number of iterations required, but this is still quite large. An iteration strategy that minimizes N_{iter} is also needed. These expenses have meant that the BEM was not used for very large problems.

The development of the fast multipole method (FMM) [4] and use of Krylov iterative methods presents a promising approach to improving the scalability of integral equation methods. The FMM allows the matrix vector product to be performed to a given precision ϵ in $O(N \log N)$ operations, and further does not require the computation or storage of all N^2 elements of the matrices, reducing the storage costs to $O(N \log N)$ as well. Incorporating this fast matrix vector product in a quickly convergent iterative scheme allows the system to be rapidly solved with $O(N_{iter}N \log N)$ cost.

The FMM for the Laplace and Helmholtz equations exploits factorized local and far-field (multipole) expansions of the Green's function obtained via the addition theorem. The basic idea of the FMM is to truncate the infinite series up to p^2 terms in 3D, and use translation operators for reexpansion of the solution about an arbitrary spatial point. The translation operators are also replaced by approximate (truncated) operators. In the original FMM the translation cost for a $O(p^2)$ representation was $O(p^4)$. Subsequent improvements lead to translation methods with costs of $O(p^3)$, $O(p^2 \log p)$ and even $O(p^2)$, though in the latter two cases the asymptotic notation hides a large constant cost. Later this method was intensively studied and extended to solution of many other problems. While the literature and previous work is extensive, reasons of space do not permit us to discuss them. We refer the reader to the comprehensive review [9].

Our particular interest is in the combination of the FMM with the BEM in 3D for solving the Laplace equation, and the Helmholtz equation at low to moderate frequencies. The case of the Helmholtz and the related Maxwell equations is somewhat more complicated, and the development of boundary-element/FMM combinations for different equations is a matter of more recent research. Of particular interest to the initial authors were relatively high frequency applications for which the FMM based on spherical expansion representations of multipoles was not competitive with direct matrix vector products. The development of diagonal translation operators [11] alleviated this difficulty. However, these made the implementation of the FMM/BEM more complex and subject to instabilities at low frequencies, and as a consequence again not too widely adopted.

Contributions of the present paper: In fact the FMM for both the Laplace and Helmholtz equations at moderate frequencies can be handled well by $O(p^3)$ translation techniques based on a decomposition of the translation to rotation and coaxial translations (see [5, 8]). As discussed earlier the FMM requires $O(N)$ or $O(N \log N)$ storage space and $O(N)$ or so operations for the matrix-vector product. While one may wonder about the accuracy of the FMM, where exactness is

sacrificed for the speed, we should emphasize, first, that in practice this accuracy can be made close to machine precision, second, that in the iteration procedures the accuracy should be consistent with the criterion to stop the iterative process, and, finally, that the accuracy of the FMM should be considered together with accuracy of the BEM technique, which employs surface approximation via discretization and approximate computation of the boundary integrals, and based on our experience introduce larger errors than the FMM does. Moreover, we note that for accurate solution of the Helmholtz equation the size of the boundary elements should be much smaller than the wavelength, which produces severe constraints for high frequency problems. Given these considerations it is possible to develop effective large scale FMM solutions. We must emphasize that several other authors (e.g., [10, 13]) have developed FMM/BEM algorithms. Here our intention is to present some aspects of our implementations. In particular our approach is characterized by the use of the Green's identity or layer potentials ("indirect" BEM), collocation techniques, Krylov iterative methods that may be preconditioned, and an overall choice of techniques that have a consistent accuracy in all aspects of the algorithm. The results of solutions of the test problems and issues related to errors and performance of the methods employed are discussed.

2 Problem formulation

We consider boundary value problems for a complex potential ϕ satisfying the Laplace or Helmholtz equations on a finite or infinite domain V in 3D, and subject to boundary conditions on S , the boundary of the domain:

$$\nabla^2 \phi = 0, \quad \nabla^2 \phi + k^2 \phi = 0, \quad \mathbf{x} \in V \subset \mathbb{R}^3, \quad k \in \mathbb{R}, \quad (1)$$

$$\alpha(\mathbf{x}) \phi(\mathbf{x}) + \beta(\mathbf{x}) q(\mathbf{x}) = \gamma(\mathbf{x}), \quad \mathbf{x} \in S, \quad q(\mathbf{x}) = \frac{\partial \phi}{\partial n}(\mathbf{x}) = \mathbf{n}(\mathbf{x}) \cdot \nabla \phi(\mathbf{x}). \quad (2)$$

Here α, β , and γ are some specified complex valued functions on S and \mathbf{n} is the exterior normal. For infinite domains we assume ϕ decays to zero for the Laplace equation and satisfies the Sommerfeld condition for the Helmholtz equation,

$$\lim_{|\mathbf{x}| \rightarrow \infty} \phi = 0, \quad \lim_{|\mathbf{x}| \rightarrow \infty} \left(|\mathbf{x}| \left(\frac{\partial \phi}{\partial |\mathbf{x}|} - ik\phi \right) \right) = 0. \quad (3)$$

Arbitrary solutions to these equations can be expressed as sums of the single and double layer potentials

$$\phi(\mathbf{y}) = \mathbf{K}(\sigma(\mathbf{x})) + \mathbf{L}(p(\mathbf{x})), \quad \mathbf{x} \in S, \quad \mathbf{y} \in V \quad (4)$$

$$\mathbf{K}(\sigma(\mathbf{x})) = \int_S \sigma(\mathbf{x}) G(\mathbf{x} - \mathbf{y}) dS(\mathbf{x}), \quad \mathbf{L}(p(\mathbf{x})) = - \int_S p(\mathbf{x}) \frac{\partial G(\mathbf{x} - \mathbf{y})}{\partial n(\mathbf{x})} dS(\mathbf{x}),$$

where σ and p are surface densities, while G is the free space Green's function for the Laplace or the Helmholtz operators:

$$G(\mathbf{x} - \mathbf{y}) = \frac{1}{4\pi |\mathbf{x} - \mathbf{y}|}, \quad G(\mathbf{x} - \mathbf{y}) = \frac{e^{ik|\mathbf{x} - \mathbf{y}|}}{4\pi |\mathbf{x} - \mathbf{y}|}, \quad (5)$$

respectively. For both equations Green's identity holds, which is equation (4) with $\sigma(\mathbf{x}) = \pm q(\mathbf{x})$ and $p(\mathbf{x}) = \pm \phi(\mathbf{x})$ (here the upper sign refers to the interior and the lower sign to the exterior problem), and which can be used to obtain ϕ in the domain if the potential and its normal derivative are known on the boundary. This leads to the integral equation

$$\pm \frac{1}{2} \phi(\mathbf{y}) = \mathbf{K}(q(\mathbf{x})) + \mathbf{L}(\phi(\mathbf{x})), \quad \mathbf{x} \in S, \quad \mathbf{y} \in S, \quad (6)$$

which can be used together with Eq. (2) for determination of the boundary values. To avoid spurious eigenvalues for the external BEM one of possibilities to resolve this is to stay within the layer potential formulation [1], which provides according to the jump conditions:

$$\phi^\pm(\mathbf{y}) = \pm \frac{1}{2} p(\mathbf{y}) + \mathbf{K}(\sigma(\mathbf{x})) + \mathbf{L}(p(\mathbf{x})), \quad \mathbf{x} \in S, \quad \mathbf{y} \in S, \quad (7)$$

$$q^\pm(\mathbf{y}) = \pm \frac{1}{2} \sigma(\mathbf{y}) + \mathbf{K}'(\sigma(\mathbf{x})) + \mathbf{L}'(p(\mathbf{x})), \quad \mathbf{x} \in S, \quad \mathbf{y} \in S,$$

$$\mathbf{K}'(\sigma(\mathbf{x})) = \frac{\partial}{\partial n(\mathbf{y})} \mathbf{K}(\sigma(\mathbf{x})), \quad \mathbf{L}'(\sigma(\mathbf{x})) = \frac{\partial}{\partial n(\mathbf{y})} \mathbf{L}(\sigma(\mathbf{x})), \quad \mathbf{x} \in S, \quad \mathbf{y} \in S. \quad (8)$$

This can be used for solution of the Helmholtz equation, with $\sigma(\mathbf{x}) = i\eta p(\mathbf{x})$, where η is some complex parameter. In this case equations (7) and (2) lead to the following single integral equation for the layer potential density

$$\alpha(\mathbf{y}) \left\{ \pm \frac{1}{2} p(\mathbf{y}) + i\eta \mathbf{K}(p(\mathbf{x})) + \mathbf{L}(p(\mathbf{x})) \right\} + \beta(\mathbf{y}) \left\{ \pm \frac{1}{2} i\eta p(\mathbf{y}) + i\eta \mathbf{K}'(p(\mathbf{x})) + \mathbf{L}'(p(\mathbf{x})) \right\} = \gamma(\mathbf{y}). \quad (9)$$

Particularly for the external (scattering) problems, which solution is unique, this avoids spurious internal resonances.

3 BEM speed up with the FMM

Several schemes of coupling the BEM with the FMM can be thought, and we also tried a few until we came to the following, rather simple scheme. A matrix-vector product of type $\mathbf{A}\mathbf{u}$ is required. \mathbf{A} is represented as

$$\mathbf{A} = \mathbf{A}_{sparse} + \mathbf{A}_{dense}, \quad (10)$$

where \mathbf{A}_{sparse} can be computed directly using standard quadratures over the element i , for elements j which are in the neighborhood of i . This neighborhood size is a user controllable parameter, and can be varied as needed. The dense part includes most pairwise interactions. As it includes only remotely located elements relatively low order quadrature can be used for them to achieve the required accuracy. Moreover, in our test implementations we used surface discretization with flat triangular elements, for which we used a constant approximation of the unknown function (potential or its normal derivative) over the panel. In this case we also can expect that the Greens function and its derivatives for relatively distant interactions can be approximated in the same way at the same accuracy, and was confirmed by our numerical experiments.

BEM and FMM data structures: Detailed description of the FMM for the Laplace and Helmholtz equations can be found elsewhere [4, 7] and here we just point out few details on the use of the FMM with the BEM. First we note that the data structure of the FMM is based on the octree space subdivision up to some level l_{max} . Selection of l_{max} is dictated by an optimization problem for FMM costs, which balances the costs of the translation and direct summation operations. Deviations from optimal l_{max} are not desirable, as they heavily influence the FMM performance [7]. On the other hand the split in (10) is dictated by the accuracy of the BEM and therefore the size of the neighborhood where we perform direct computations of integrals may not coincide with the sizes of neighborhoods at different levels of the FMM. Our numerical tests show that (fortunately) the size of the neighborhood at the optimal maximum space subdivision level is larger than the size required for direct integral evaluations. This means that all elements which intersect the neighborhood of an element i at the finest level, and whose contribution to the potential at the element center can be classified into two sets. First are the elements j that are closer than some distance r_{min} from the center of i to the closest corner of j . The contribution of these elements is performed using higher order quadrature or special integral treatment (for singular and hypersingular integrals) as in the conventional BEM. The second set of elements are located further than r_{min} . Their contribution is taken into account using low order quadrature, as they are remote in the sense of BEM, but close in the sense of the FMM.

Iterative methods: The basic iterative method we used is the Generalized Minimal Residual Method (GMRES) and its modifications (flexible GMRES, fGMRES) [12], which allow the use of various FMM-based preconditioners [6]. In all cases for the Laplace equation and for the Helmholtz equation at low frequencies unpreconditioned GMRES showed good results, while the convergence rate of this method for the Helmholtz equation substantially reduces at higher frequencies.

Computation of normal derivatives in the FMM: Eq. (9) requires four matrix-vector products, and the use of Eq. (6) requires two matrix-vector products (in the case of mixed boundary conditions). These can be performed by the FMM in a single run, as for a single matrix-vector product. Indeed, the first step of the regular FMM is to build multipole expansions about the centers of the source boxes, \mathbf{x}_* . We handle this step using expansions of Greens function over the multipole basis functions $S_n^m(\mathbf{r})$:

$$G(\mathbf{y} - \mathbf{x}) \approx \sum_{n=0}^{p-1} \sum_{m=-n}^n C_n^m S_n^m(\mathbf{y} - \mathbf{x}_*), \quad C_n^m = C_n^m(\mathbf{x}, \mathbf{x}_*), \quad (11)$$

where p is the truncation number, and expressions for coefficients C_n^m for the Laplace and Helmholtz equations can be found elsewhere [7, 8]. We compute the normal derivative of arbitrary function $F(\mathbf{x})$, which can be expanded into a series over the basis functions with coefficients $\{C_n^m\}$ using sparse-matrix differential operators $\{D_{nn'}^{mm'}\}$:

$$\mathbf{n} \cdot \nabla_{\mathbf{x}} F(\mathbf{x}) \approx \sum_{n=0}^{p-1} \sum_{m=-n}^n B_n^m S_n^m(\mathbf{y} - \mathbf{x}_*), \quad \{B_n^m\} = \{D_{nn'}^{mm'}(\mathbf{n})\} \{C_{n'}^{m'}\}, \quad B_n^m = \sum_{n=0}^{p-1} \sum_{m=-n}^n \sum_{n'=0}^{p-1} \sum_{m'=-n'}^{n'} D_{nn'}^{mm'} C_{n'}^{m'}. \quad (12)$$

Expressions for $D_{nn'}^{mm'}$ for the Helmholtz equation can be found in [7], while for the Laplace equation can be derived from relations in [3]. Therefore far field expansions of the boundary integrals can be written as

$$\begin{aligned} & \sigma_j \int_{S_j} G(\mathbf{y} - \mathbf{x}) dS(\mathbf{x}) + p_j \int_{S_j} \mathbf{n} \cdot \nabla_{\mathbf{x}} G(\mathbf{y} - \mathbf{x}) dS(\mathbf{x}) \\ & \approx \sigma_j \sum_{q=1}^Q w_q^{(j)} G(\mathbf{y} - \mathbf{x}_q^{(j)}) + p_j \sum_{q=1}^Q w_q^{(j)} \mathbf{n}_j \cdot \nabla_{\mathbf{x}} G(\mathbf{y} - \mathbf{x}_q^{(j)}) \approx \sum_{n=0}^{p-1} \sum_{m=-n}^n A_n^{(j)m} S_n^m(\mathbf{y} - \mathbf{x}_*), \\ & A_n^{(j)m} = \sum_{q=1}^Q w_q^{(j)} \left(\sigma_j C_n^m(\mathbf{x}_q^{(j)}, \mathbf{x}_*) + p_j B_n^{(j)m}(\mathbf{x}_q^{(j)}, \mathbf{x}_*) \right), \quad \{B_n^m\} = \{D_{nn'}^{mm'}(\mathbf{n}_j)\} \{C_{n'}^{m'}\}, \end{aligned} \quad (13)$$

where Q is the order of quadrature over the boundary element S_j with weights $w_q^{(j)}$ and abscissas $\mathbf{x}_q^{(j)}$. A similar situation holds at the evaluation step if using the method of layer potentials, where derivatives $\mathbf{n}(\mathbf{y}) \cdot \nabla_{\mathbf{y}}$ can be computed using respective sparse-matrix differential operator on the expansion coefficients.

4 Laplace equation

Performance tests for the Laplace equation were conducted for multiparticle geometries of type shown in Fig. 1. Analytical solution was generated as a sum of monopoles placed at the center of each ellipsoid, which total intensity was 1. The Dirichlet problem was solved using the BEM and the obtained normal derivatives were compared with the analytical values to evaluate the error of the numerical method. The function values and normal derivatives were computed at mesh vertices (using standard averaging over the elements containing the same vertex), which number is referred further as N (the number of elements was approximately twice larger).

Four methods implemented in Fortran 90 in double precision and compared. First, we used standard BEM, where the BEM matrices were computed, stored, and the linear system resulting from Green's identity was solved using LU-decomposition from LAPACK. Second, the BEM matrices were computed and stored, while unpreconditioned GMRES (CERFACS software available online) was used for iterative solution of the resulting system with a prescribed error $\epsilon = 10^{-5}$ for termination of the process. We checked that in all cases this was sufficient to provide the same error in the numerical solution (relative error of order 10^{-2}). The first two methods require $O(N^2)$ memory for storage of the BEM matrices, and our computational resources limited us to compute problems of size smaller than $N \simeq 10^4$. The other two methods tested required only $O(N)$ memory and so could be used for computation of larger problems on the same computer. Method 3 was the same as Method 2 with the only difference that the entries of the BEM matrices were recomputed each time the matrix-product was requested, thereby avoiding storage. The last method used combined the same GMRES with the same termination error and the FMM for matrix-vector multiplication, where we used truncation number $p = 8$ for all cases. We checked that the error of solution was practically the same for $N \lesssim 10^4$ as for other methods, while for larger N the error decays and stays within the range 10^{-2} - 10^{-4} . Higher accuracy ($\sim 10^{-6}$) was achievable for larger N by increasing p and decreasing ϵ .

Fig. 2 shows that the CPU times for methods 1-4 are scaled approximately as $O(N^3)$, $O(N^2)$, $O(N^2)$, and $O(N)$, respectively, which is consistent with the theory assuming that the number of iterations does not change with N . In fact, the number of iterations do increase slowly with N as shown in Fig. 2 right, which explains deviation of the total CPU time from the linear dependence at larger N . The number of iterations was the same for methods 2-4, except for $N = 488$ where the first two methods converged for 10 iterations, while the FMM-based needed 13 iterations. For $N = 843,264$ (1,679,616 elements, 1728 ellipsoids) the number of iterations was 31 (total CPU time for solution 28 min 19 s, which includes precomputations of the near element interactions, preset of the FMM, and the iterative process with 48 s per matrix vector multiplication).

5 Helmholtz equation

The tests of the BEM for the Helmholtz equation were performed by solution of acoustic scattering problems off objects of different shape. The objects were sound-hard leading to an external Neumann problem for the scattered field. As a test we selected scattering of the plane incident wave from a single sphere, which has an analytical solution in the form of the infinite series (due to Lord Rayleigh, can be found elsewhere, e.g. [7]). These series can be appropriately truncated and the error of the solution can be accurately estimated. We performed tests using the same four methods as reported for the Laplace equation, plus we compared solutions obtained using boundary integral equations resulting from the layer potential and Green's identity. Also some tests using the fGMRES with different preconditioners were performed.

In this paper we report only results obtained using the unpreconditioned GMRES and Green's identity. Fig. 3 shows scattering off a sphere. The numerical solution reproduces fine oscillating structure of the acoustic field near the point $\theta = 180^\circ$ which happens at large ka , where a is the sphere radius. Even the use of high frequency mesh with 480,000

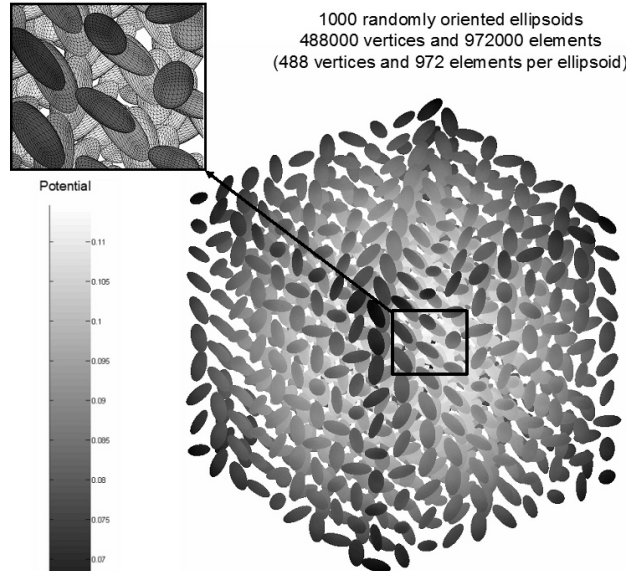


Figure 1: Geometry of the test problems for performance tests for the Laplace equation. Centers of M^3 equal ellipsoids were placed on a cubic grid and each ellipsoid was randomly rotated.

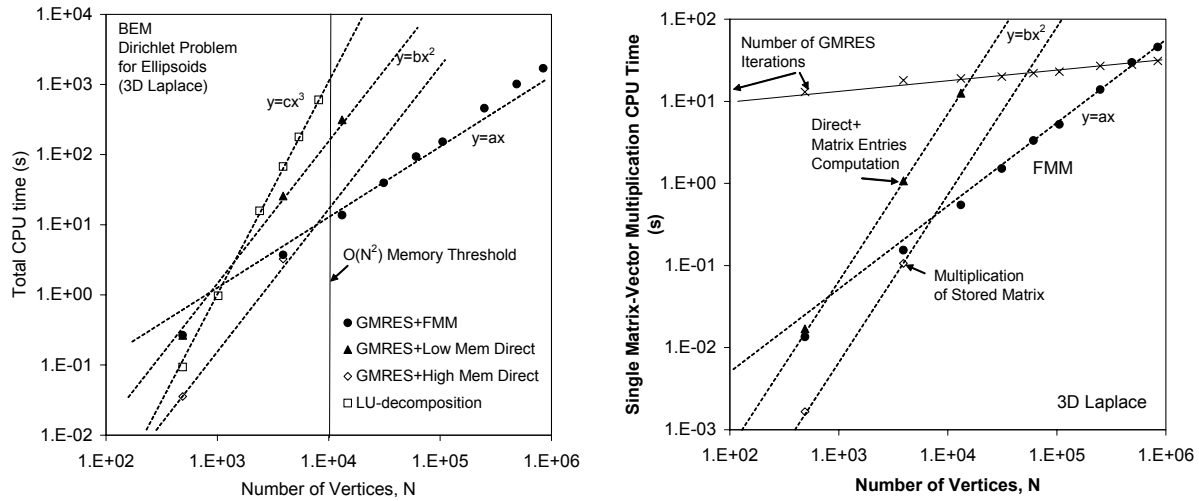


Figure 2: *Left*: Performance of the 4 BEM methods for the Dirichlet problem for the Laplace equation on the domain with a collection of ellipsoids shown in Fig 1. *Right*: CPU time for a single matrix vector multiply. Between 13 and 31 iterations are needed for convergence and are indicated via crosses. (Intel Xeon 3.2 GHz processor with 3.5 GB RAM.)

elements for $ka = 30$ provided $k\delta = 0.4$, where δ is the size of the largest boundary element (about 16 elements per wavelength). Computations of this were performed with 6 levels of the octree with maximum truncation number $p = 22$ at level 2, and convergence to error $\epsilon = 10^{-5}$ took 115 iterations.

The CPU time required for solution of the problem with $ka = 10$ using different methods is shown in Fig. 4. As the kD for different N is fixed ($kD = 34.64$) the methods as in the case of the Laplace equation show scaling close to $O(N^3)$, $O(N^2)$, $O(N^2)$, and $O(N)$, respectively. In the reported case the accuracy of the solution was 0.15 for case $N = 1016$, was $\approx 10^{-2}$ for $N \sim 10^4$ and dropped to $\sim 10^{-4}$ for $N \sim 10^6$ despite the maximum truncation number used in the FMM ($p = 12$) and the GMRES termination criteria ($\epsilon = 10^{-5}$) were the same. This change in the accuracy is due to two factors, first, for the low frequency mesh parameter $k\delta$ was large enough, and second, that finer mesh approximated the sphere better. In contrast to the Laplace equation the number of iterations slightly decreased at increasing N (see Fig. 4 right). This explains the deviation of the total CPU time below the linear asymptote, as the CPU time for the FMM matrix vector product scales almost linearly (Fig. 4 right). For $N \gtrsim 10^3$ direct matrix vector product with recomputation of matrix elements was slower. Note that the FMM for the Helmholtz equation is slower than for the Laplace equation since for the Helmholtz case all variables are complex.

Finally we applied the software for solution of some scattering problems related to hearing. This requires solution of the Helmholtz equation in domains with complex boundaries, such as a human or animal head, and ears for a range of audible frequencies, in the range $kD \lesssim 100$, for which the developed BEM/FMM works well. Parameters such as sound pressure or head related transfer functions (HRTF) are computed. Fig. 5 provides one such case. (A color movie visualizing scattering can be viewed online on the web sites of the authors.)

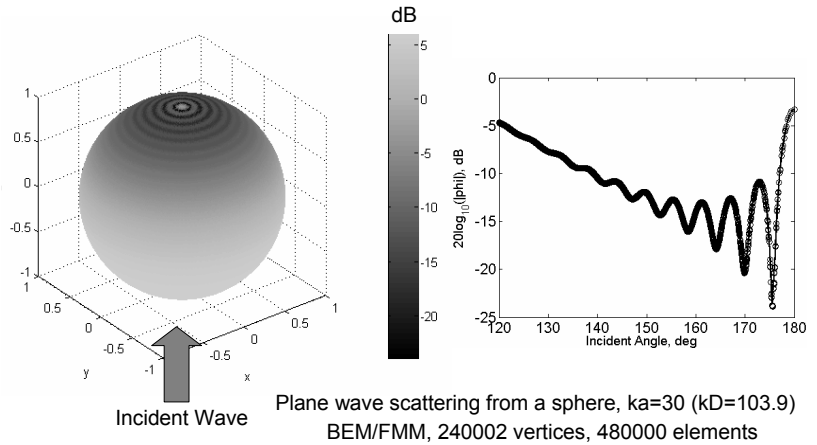


Figure 3: Scattering of a plane wave from a sound-hard sphere. The incidence angle is 0 for the front point and 180° for the rear point.

References

- [1] Chen, L.H and Zhou, J. (1992) *Boundary Element Methods*. Academic Press.

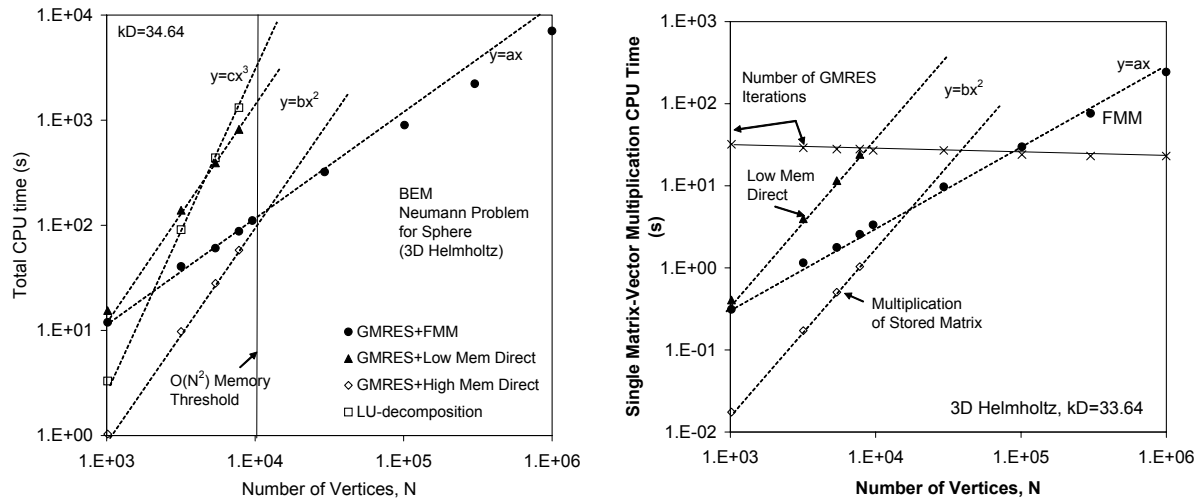


Figure 4: *Left*: CPU time for computation of scattering off a sphere in a domain of size $kD = 34.64$ as a function of the degrees of freedom. *Right*: Dependence of the matrix vector multiplication time for the Helmholtz equation on the number of degrees of freedom for the case on the left. The crosses show the number of iterations.

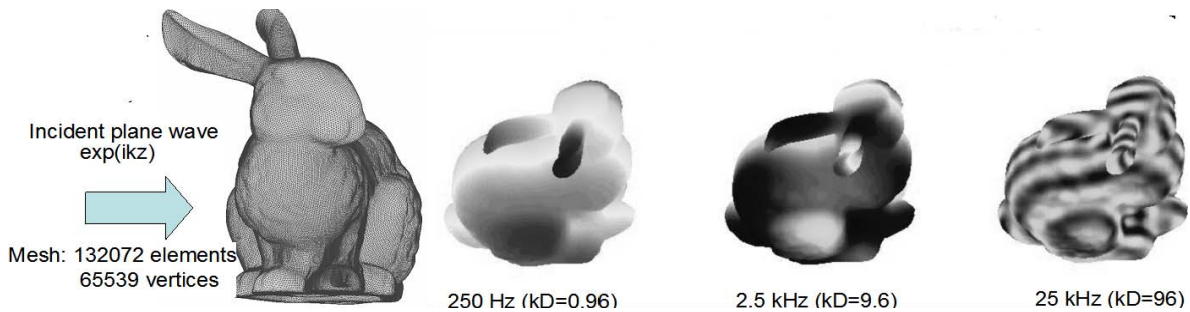


Figure 5: An example of computation of sound scattering from bunny model using the BEM/FMM. The sound pressure for different frequencies at some moment of time is shown on the bottom pictures.

[2] Colton, D. and Kress, R. 1998 *Inverse Acoustic and Electromagnetic Scattering Theory*. 2nd. ed. Berlin: Springer..

[3] M.A. Epton and B. Dembart, Multipole translation theory for the three-dimensional Laplace and Helmholtz equations, *SIAM J. Sci. Comput.*, 16(4), 1995, 865-897.

[4] Greengard, L. (1988). *The Rapid Evaluation of Potential Fields in Particle Systems*. (MIT Press, Cambridge, MA).

[5] Gumerov, N.A., and Duraiswami, R. (2003). "Recursions for the computation of multipole translation and rotation coefficients for the 3-D Helmholtz equation," *SIAM J. Sci. Stat. Comput.* 25(4), 1344-1381, 2003.

[6] Gumerov, N.A. and Duraiswami, R. (2005). "Computation of scattering from clusters of spheres using the fast multipole method," *J. Acoust. Soc. Am.*, 117 (4), Pt. 1, 1744-1761.

[7] Gumerov, N.A. and Duraiswami, R. (2005) *Fast Multipole Methods for the Helmholtz Equation in Three Dimensions*. (Elsevier, Oxford, UK).

[8] Gumerov, N.A. and Duraiswami, R. (2005) "Comparison of the efficiency of translation operators used in the fast multipole method for the 3D Laplace equation, Technical Report UMIACS-TR-#2005-09, University of Maryland.

[9] N. Nishimura, Fast multipole accelerated boundary integral equation methods, *Appl Mech* .55 (2002) 299-324.

[10] Ramaswamy D, Ye W, Wang X, and White J (1999), Fast algorithms for 3-D simulation, *J. Modeling Simulation of Microsystems*, 1, 77-82.

[11] Rokhlin, V. (1993). "Diagonal forms of translation operators for the Helmholtz equation in three dimensions," *Appl. and Comp. Harmonic Analysis*, 1, 82-93.

[12] Saad, Y.(1993). "A flexible inner-outer preconditioned GMRES algorithm," *SIAM J. Sci. Comput.* 14(2), 461-469.

[13] Sakuma, T. and Yasuda, Y. (2002). Fast multipole boundary element method for large-scale steady-state sound field analysis, part i: Setup and validation. *Acustica/Acta Acustica*, 88:513-525.